Machine-learning Skyrmions

Vinit Kumar Singh[1,*] and Jung Hoon Han[2,†]

[1] *Department of Physics, Indian Institute of Technology, Kharagpur 732102, India*
[2] *Department of Physics, Sungkyunkwan University, Suwon 16419, Korea*

(Dated: June 2, 2018)

Introduction: The basic idea behind teaching machine learning (ML) algorithm to recognize various phases of many-body systems, whether classical or quantum, is to input the many-body configuration together with an "answer" to the phase to which it belongs. After such supervised learning is implemented successfully, the ML algorithm can recognize a new input configuration, not drawn from the previous training set, as belonging to a certain phase, say A or B. If the input is drawn from states close to some phase transition, the prediction will be either A or B phase with certain probability distribution. The continuous change in the probability with temperature or tuning parameter for different system sizes can be used to correctly identify the critical temperature (classical phase transition) or the interaction strength (quantum phase transition). Most studies in the recent years along this line of thinking have focused on the transition between ordered and disordered phase, with a second-order critical point separating them. For first-order phase transition, the prediction changes abruptly from 100% A to 100% B across the critical point. Following a natural progression, models that were studied with the ML method have evolved from Ising[1–6] to XY[4,7,8] spins, and most recently to Heisenberg[9] spins.

Here we address various aspects of the Heisenberg-Dzyaloshinskii-Moriya-Zeeman (HDMZ) spin Hamiltonian by the ML method:

$$H_{\rm HDMZ} = -J\sum_{i\in L^2}\mathbf{n}_i\cdot(\mathbf{n}_{i+\hat{x}}+\mathbf{n}_{i+\hat{y}}) + D\sum_i(\hat{y}\cdot\mathbf{n}_i\times\mathbf{n}_{i+\hat{x}} - \hat{x}\cdot\mathbf{n}_i\times\mathbf{n}_{i+\hat{y}}) - \mathbf{B}\cdot\sum_i\mathbf{n}_i. \quad (1)$$

This lattice model, usually solved in two-dimensional $L\times L$ square lattice, is known to describe the magnetic interaction at the interface of a magnetic layer with a non-magnetic layer, or a magnetic layer exposed to vacuum. Its phase diagram, by now well-known, includes the skyrmion crystal over some intermediate field range, flanked by spiral phase at low field and ferromagnetic phase at high field[10–14].

Classifying intermediate phases: As an initial application of the ML ideas to the study of the HDMZ model and its phases, we created a training set of configurations drawn from deep inside the spiral, skyrmionic, and ferromagnetic phases of the model (1) by the Monte Carlo (MC) method. The training data was initially prepared in terms of spin angles (θ_i,ϕ_i), which gave far poorer results than if the data was prepared in terms of the magnetization $\mathbf{n}_i = (\sin\theta_i\cos\phi_i, \sin\theta_i, \sin\phi_i, \cos\theta_i)$. All the ML analysis presented in this paper is thus based on the magnetization inputs. Only its z-component was used for training in earlier work[9].

After training, the validation procedure gave nearly 100% correct values for the phase labels. This is not surprising given the fact that validation sets also came from deep inside one of the three phases. The next logical step is to generate configurations that have mixed characters and ask the ML program to predict the phases to which they belong. It is well-known both experimentally and from simulations that a substantial mixed phase or intermediate phase region exists in two dimensional skyrmion matter[15]. They are mixed spiral and skyrmion (SpSk) regions at low fields, and mixed skyrmion and ferromagnetic (SkFm) regions at higher fields. Because of their presence, a sharp phase boundary separating one phase from another is difficult to define. The ML prediction is expected to reflect this degree of uncertainty.

Our training set was generated on 24×24 lattice with $D/J = \sqrt{6}$, corresponding to the spiral period $\lambda = 6$. The inter-skyrmion distance in the skyrmion phase is also of the same order, giving rise to the nucleation of about $(L/\lambda)^2$ number of skyrmions. The average spin chirality distribution [see (2) for definition] over the (T, B) plane is presented in Fig. 1. Judging from the lack of spin chirality, the $B = 0.5$ line over the temperature $T\in[0, 0.25]$ can be said to clearly belong to the spiral phase. Likewise, one can say with confidence that $B = 2.5$ over $T\in[0, 0.25]$ belongs to the ferromagnetic phase. The robust skyrmion phase can be found at $B = 2.0$. For each B, the temperature interval was divided into ?? steps and 50 equilibrium configurations were generated by MC annealing. Using the total of 6,000 configurations thus obtained for training, we then generate a new batch of MC configurations at $T = 0.1$ and $B\in[1.0, 1.5]$, which admittedly belongs to the SpSk mixed phase, and another batch at $T = 0.5$ and $B\in[2.5, 3.0]$ belonging to the SkFm mixed phase. They are then fed to the trained

ML algorithm to make prediction regarding its phase as spiral, skyrmionic, or ferromagnetic. Recall that we were using them as labels in the training protocol, in the hope that the machine will learn to recognize the phase labels for each input configuration properly. Naively, a mixed phase configuration is expected to get one label at x fraction of the time, and the other label for the other $(1-x)$ fraction. After all, this is how one describes the mixed phase in thermodynamics, in terms of the volume fraction of each phase.

Figures 2 and 3 show the probability distribution of the ML-predicted labels for mixed-phase configurations. At each B, several hundred configurations were tested for their labels, and the numerical average of the answers given by the machine is plotted. The sum of the probabilities must add to one. As the volume fraction changes smoothly over the course of the mixed-phase evolution, the probability for predicting one phase must decrease continuously, giving way to a smoothly increasing probability to predict the other phase. The actual test results are wildly different. Even though extremely fine steps were taken between adjacent magnetic fields, the program failed to recognize the continuous nature of the evolution within the mixed phase. Neither increasing the number of test configurations (to eliminate the statistical error) nor the training configuration (for a more unbiased training) helped improve the prediction to a smoother form. In an analogous attempt on a vast array of models exhibiting second-order phase transition, the ML program trained solely on the configurations deep inside the ordered and disordered phases could successfully predict the phases near the critical temperature (or the critical interaction coupling) in a continuously varying manner. According to our experiment, the ML program trained on the three distinct phases of the skyrmion model fails to make continuously varying predictions for its mixed phases.

Given the cryptic nature of the ML training, the precise reason for the failure is difficult to point out. The ML architecture we used involved the initial CNN layer with ..., followed by ?? neural network layers of sizes xx, xx, and xx, etc. Changes in the architecture also failed to improve the final results. It appears that models that exhibit an extended mixed phase region must be trained in a different manner from those models with a sharp second-order phase transition point. This problem is taken up next.

Feature predictions: The main characteristics of the ferromagnetic and the skyrmion phases are the average magnetization and the chirality, respectively, defined as (N=number of lattice sites)

$$m = (1/N)\sum_i n_i^z,$$
$$\chi = (1/N)\sum_i (\mathbf{n}_i \cdot \mathbf{n}_{i+\hat{x}} \times \mathbf{n}_{i+\hat{y}}). \qquad (2)$$

The spiral phase is the one where none of these features takes on significant values. Instead of training the algorithm on the "labels" of the phases as spiral, skyrmion, or ferromagnet, we might train it on their features such as m and χ. Once the ML algorithm could be trained to correctly predict such values for input configurations, the problem of labeling them is as good as solved, since an input whose m (χ) is predicted to be close to the maximum allowed value can have no other label than ferromagnet (skyrmion). Intermediate values of m and χ signify the SkFm mixed phase. Finally, a configuration with small but non-negligible χ and m are likely associated with the SpSk mixed phase. In other words, the labeling problem is delegated to the human decision, while the machine is left to do its best work at predicting quantitative features of the input.

We carried out supervised learning of the (m, χ) features on the configurations from a wide temperature range $0 < T \leq 2.0$ and magnetic field $0 \leq B \leq 3.5$. For each (T, B) we collect 100 MC-annealed configurations for training purpose. The temperature and magnetic field intervals were sufficiently fine, as one can see from the high quality of the pre-smearing data of the calculated chirality in Fig. 1 obtained from the same training set. After training, those configurations not included in the training set are used to compare the machine-predicted (m, χ, T, B) against the actual values. As shown in Figs. 4 and 5, the agreement between predicted and actual values is very good across the whole phase diagram.

Encouraged by the success of the feature prediction in terms of m and χ, we next ask if the machine can be trained to recognize the particular temperature (T) and magnetic field (B) values from which the configuration originated. Under the hypothetical circumstance when the person doing the calculation failed to record the (T, B) values for his vast number of MC configurations, such machine could serve as a useful recovery tool. A similar ML-aided recovery procedure might serve the experimentalist in recovering features of the vast array of data they had once taken and forgotten to label with conditions under which the data was taken. After the training on (T, B) values of the input, the predicted values for them came very close to the actual ones as shown in Figs. 6 and 7. **Quantify the differences, describe the architecture used.**

Prediction for adiabatically connected phases: The HDMZ Hamiltonian (1) represents the simplest case of spin interaction that supports the skyrmion phase. Various modifications can be added to it, and one that reflects the disorder in the actual material is given by

$$H_K = -K \sum_{i \in \text{random}} (S_i^z)^2. \qquad (3)$$

The magnetic anisotropy term of strength K is added at the random sites occupying a fraction p of the whole

lattice. The model $H(K,p) = H_{\rm HDMZ} + H_K$ represents an adiabatically connected family of Hamiltonians as long as K is sufficiently small compared to other energy scales. It is interesting to ask whether the ML algorithm, trained solely on the configurations drawn from $H(0,0) = H_{\rm HDMZ}$, can have predictive power over those generated from arbitrary $H(K,p)$. It is also a pragmatic question, when it comes to addressing the machine's predictive power over the experimental data. The real materials are never as simple as the HDMZ Hamiltonian, and there is always some degree of disorder one does not know a priori. If the model Hamiltonian used for training is somehow adiabatically connected to the real Hamiltonian governing physical systems, one expects the predictive power of the ML to hold sway over the real-life data as well.

A large number of configurations at $K = 0.5$ and $p = 0.5$ were generated by MC and tested by the ML algorithm, which was trained solely on the pristine Hamiltonian $H_{\rm HDMZ}$. As shown in Figs. 8, 9, very good fits of all features (m, χ, T, B) were obtained, in a nice demonstration of the adiabatic continuity of the ML's predictive power. Another test was conducted on configurations generated by $H(0.5, 1)$, which is the anisotropic version of the HDMZ Hamiltonian without disorder. The results are ....

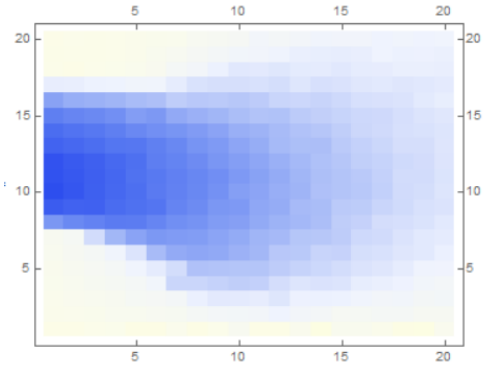

FIG. 1. Chirality distribution in the (T, B) plane.

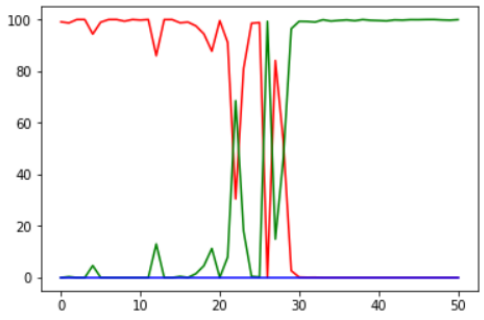

FIG. 2. Phase label probabilities for SpSk mixed phase.

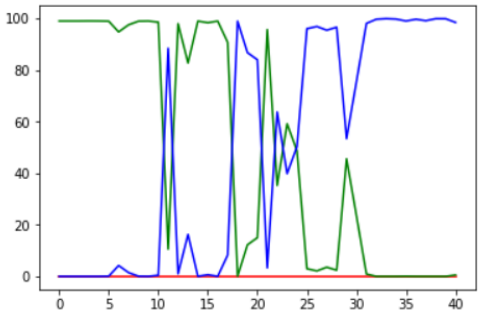

FIG. 3. Phase label probabilities for SkFm mixed phase.

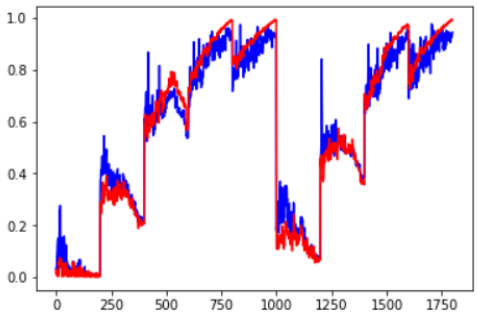

FIG. 4. Fit of the machine-predicted magnetization to the actual values.

ACKNOWLEDGMENTS

This work was supported by Samsung Science and Technology Foundation under Project Number SSTF-BA1701-07.

* Electronic address: vinitsingh911@gmail.com
† Electronic address: hanjh@skku.edu

[1] L. Wang, Phys. Rev. B **94**, 195105 (2016).
[2] J. Carrasquilla and R. G. Melko, Nat. Phys. **13**, 431 (2017).
[3] A. Tanaka and A. Tomiya, J. Phys. Soc. Jpn. **86**, 063001 (2017).
[4] W. Hu, R. R. P. Singh, and R. T. Scalettar, Phys. Rev. E **95**, 062122 (2017).

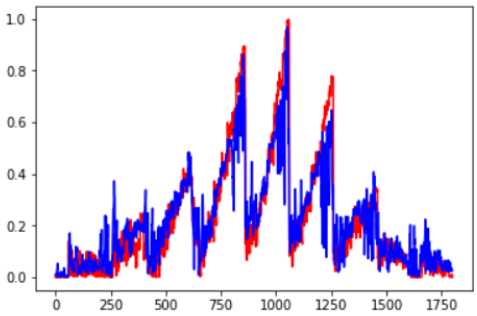

FIG. 5. Fit of the machine-predicted chirality to the actual values.

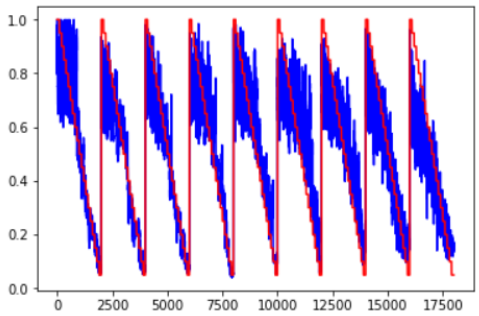

FIG. 6. Machine prediction of T against the actual temperature.

[5] S. J. Wetzel and M. Scherzer, Phys. Rev. B **96**, 184410 (2017).
[6] D. Kim and D.-H. Kim, arXiv:1804.02171v1 (2018).
[7] C. Wang and H. Zhai, Phys. Rev. B **96**, 144432 (2017).
[8] M. J. S. Beach, A. Golubeva, and R. G. Melko, Phys. Rev. B **97**, 045207 (2018).
[9] I. A. Iakovlev, O. M. Sotnikov, and V. V. Mazurenko, arXiv:1883.06682v1 (2018).
[10] N. Nagaosa and Y. Tokura, Nature Nanotech. **8**, 899 (2013).
[11] J. P. Liu, Z. Zhang, and G. Zhao, *Skyrmions: topological structures, properties, and applications* (CRC Press, 2016)
[12] W. Jiang, G. Chen, K. Liu, J. Zang, S. G. E. Velthuis, and A. Hoffmann, *Phys. Rep.* **704**,1 (2017).
[13] A. Fert, N. Reyren, and V. Cros, Nature Reviews Materials **2**, 17031 (2017).
[14] J. H. Han, *Skyrmions in Condensed Matter* (Springer, 2017).
[15] X. Z. Yu, Y. Onose, N. Kanazawa, J. H. Park, J. H. Han, Y. Matsui, N. Nagaosa, and Y. Tokura, Nature (London) **465**, 901 (2010).

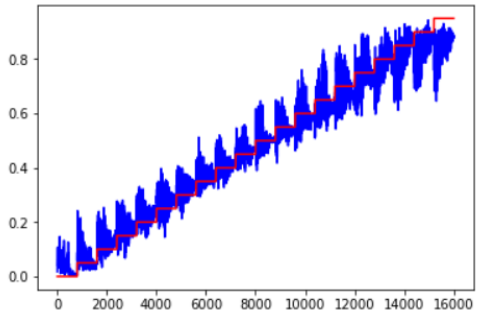

FIG. 7. Machine prediction of B against the actual temperature.

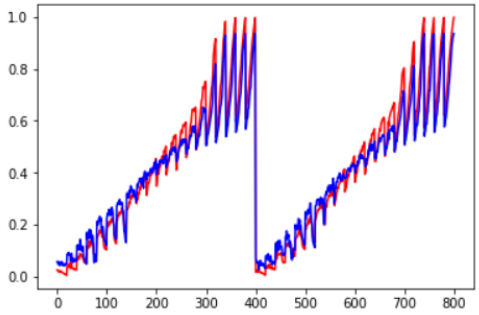

FIG. 8. Machine prediction for magnetization of the 50% disordered model configurations.

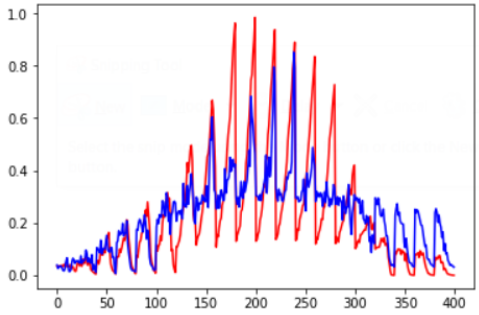

FIG. 9. Machine prediction for chirality of the 50% disordered model configurations.

FIG. 10. Machine prediction for temperature of the 50% disordered model configurations.

FIG. 11. Machine prediction for magnetic field of the 50% disordered model configurations.